BIO DESIGN

pISSN 2288-6982 | eISSN 2288-7105

TECHNICAL REPORT P 62-67

Improvement of crystal quality for X-ray diffraction of the problematic redox protein complex, thioredoxin and thioredoxin-interacting protein

Jungwon Hwang and Myung Hee Kim*

Infection and Immunity Research Center, Korea Research Institute of Bioscience and Biotechnology, Daejeon 305-806, Korea.
*Correspondence: mhk8n@kribb.re.kr

Thioredoxin-interacting protein (TXNIP) regulates many biological processes by interacting with thioredoxin (TRX) in a redox-dependent fashion. Thus, elucidation of the mechanism, by which these two proteins interact, is a key to understand redox-dependent cell signaling. Recently, the TXNIP-TRX complex structure and their interacting mechanism have been published. Both TRX (containing 5 cysteine residues) and TXNIP (containing 11 cysteine residues) are highly redox-sensitive proteins, and are therefore extremely difficult to handle *in vitro*. Here, we present details of how these problematic redox proteins can be expressed, purified, and crystallized to a suitable quality for X-ray diffraction. Both proteins were expressed as a soluble complex in the *E. coli* Rosetta-gami (DE3) system in which disulfide bonds can form owing to trxB/gor mutation. Moreover, catching TXNIP in an intermediate state, in which TRX was bound, was crucial to obtain stable complex proteins linking to crystallization.

INTRODUCTION

Thioredoxin (TRX) is a redox-active protein that is ubiquitously expressed in humans. It is one of the defense proteins that are induced in response to various oxidative stresses (Yoshihara et al., 2010). In this role, TRX is crucial for modulating intra- and extra-cellular signaling pathways, regulating a number of transcription and translation factors, and controlling the immune response (Lillig and Holmgren, 2007). Since its discovery (Tagaya et al., 1989), human TRX has emerged as an attractive target for anti-cancer drugs due to its association with many key aspects of cancer, including increased cell growth and proliferation, resistance to cell death, and increased angiogenesis (Powis and Kirkpatrick, 2007; Mukherjee and Martin, 2008).

Thioredoxin-interacting protein (TXNIP), also known as vitamin D_3 up-regulated protein-1 and thioredoxin-binding protein-2, is the only known endogenous negative regulator of TRX. Recently, the TRX-dependent and -independent functions of TXNIP have been highlighted as a regulator of cell growth, cell proliferation, and metabolism and as a modulator of the inflammatory response (Spindel et al., 2012). The TRX-dependent functions of TXNIP are achieved via inhibition of TRX activity through the formation of a stable mixed-disulfide bond between the two proteins (Patwari et al., 2006). This interaction is implicated in the significantly reduced ability of TRX to interact with a number of cellular molecules, leading to modulation of signaling. Thus, inhibition of TRX by TXNIP has emerged as one of the most important regulatory systems involved in the pathogenesis of many cancers and metabolic diseases (Spindel et al., 2012; Schulze et al., 2004; Dunn et al., 2010).

Furthermore, TXNIP is an essential ligand for the Nod-like receptor protein 3 (NLRP3) inflammasome (Zhou et al., 2010), which activates proinflammatory caspase-1 and triggers the maturation and secretion of cytokines such as interleukin (IL)-1β that are frequently associated with tumor progression (Schutze et al., 1998) and metabolic disease (Schroder et al., 2010; Choi and Nakahira, 2011). Under normoxic conditions, TXNIP is bound to TRX and inhibits the reducing activity of TRX. During oxidative stress, reactive oxygen species induce dissociation of TXNIP from TRX and the released TXNIP binds to and activates NLRP3, leading to secretion of IL-1β (Zhou et al., 2010).

From these studies, it has become evident that knowledge of the TRX-TXNIP regulatory system and TXNIP itself is central to understanding the pathogenesis of many cancers and metabolic syndromes. Many efforts have been directed to deciphering the properties of TXNIP at the molecular level (Alvarez, 2008) and the mechanism by which TXNIP regulates TRX (Patwari et al., 2006). However, the molecular characteristics of TXNIP and the molecular mechanism underlying TRX regulation by TXNIP remain largely unknown due to the lack of structural information.

We recently reported the crystal structure of the heterodimeric TRX-TXNIP complex and its regulatory mechanism (Hwang et al., 2014). Both TRX (containing 5 cysteine residues) and TXNIP (containing 11 cysteine residues) are highly redox-sensitive pro-

teins (Figure 1a) and are extremely difficult to handle *in vitro*. Therefore, this previous structural study was completed through trial and error. In this report, we describe the details of the expression, purification, and crystallization of this problematic redox protein complex for structural biology studies.

RESULTS AND DISCUSSION

Expression of the stable TXNIP-TRX complex

Human full-length TXNIP was cloned into pHis-parallel1 with an N-terminal hexahistidine tag, pGST-parellel1 with an N-terminal glutathione S-transferase tag, and pMBP-parellel1 with an N-terminal maltose-binding protein tag, for expression in *E. coli*. No soluble TXNIP protein was expressed using these fusion plasmids. A conserved domain analysis revealed that TXNIP contains N-terminal and C-terminal tandem arrestin-like domains (referred to as N-TXNIP and C-TXNIP, respectively) ranging from about amino acid (aa) 1 to 317 (Figure 1a). Thus, we deleted a non-structural C-terminal region (aa 318–391) of TXNIP, and a truncated TXNIP fragment, ranging from aa 3 to 317 (T-TXNIP), was cloned into the same vectors as were initially used for full-length TXNIP. These plasmids did not provide suitable soluble proteins. To induce expression of soluble T-TXNIP, its interacting protein, human TRX, was inserted downstream of the C-terminus of T-TXNIP (Figure 1b). The expression of this plasmid was tested in *E. coli* strains including BLR(DE3), BL21 star(DE3), C41(DE3), and C43(DE3), and this resulted in the expression of insoluble T-TXNIP and soluble TRX (data not shown). Patwari *et al*. demonstrated that the Cys32 residue of TRX and the Cys247 residue of TXNIP form a mixed disulfide bond (Patwari et al., 2006). We thus employed *E. coli* Rosetta-gami (DE3) system, in which disulfide bonds can form owing to *trxB*/*gor* mutations and consequently expression of eukaryotic proteins is improved, and both proteins were expressed as a soluble complex (Figure 1c). This indicates that TRX is tightly regulated by its interacting partner TXNIP and

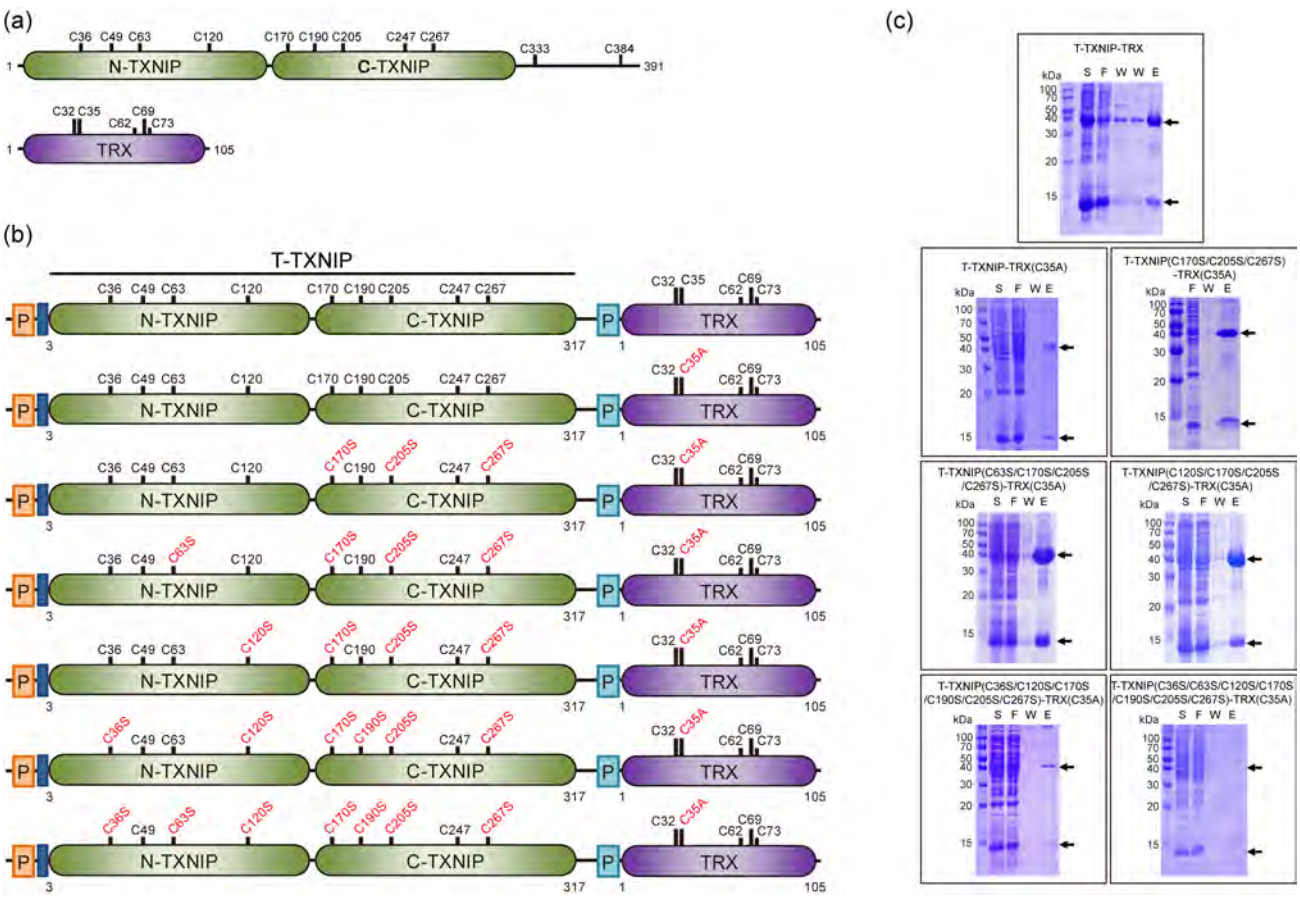

FIGURE 1 | Schematic representation of the TXNIP and TRX constructs used in this study. (a) TXNIP is shown in green and TRX is shown in purple. The locations of cysteine residues are indicated. (b) Co-expression constructs used for the expression of the TXNIP-TRX complex and its variants. The mutated residues are indicated in red. Light salmon and light blue boxes are the sites of the trc promoter and the T7 promoter, respectively. The blue box is the N-terminal hexahistidine tag containing the rTEV protease cleavage site. (c) Expressions of the T-TXNIP-TRX complex and its variants in *E. coli* Rosetta gami (DE3) cells. The expression results were analyzed by SDS-PAGE. The expressed complexes were investigated further by Ni-NTA agarose column chromatography. S, soluble fraction; F, flow-through fraction; W, washing fraction; E, eluted fraction. The upper arrows indicate T-TXNIP and its variants, and the lower ones indicate TRX and its variant.

that disulfide bond formation is critically involved in this interaction. Another problem we faced in obtaining the stable protein complex was that TRX dissociated from T-TXNIP during purification. To catch TXNIP in an intermediate state in which TRX was bound, the complex needed to be stabilized. Consequently, the active Cys35 residue of TRX was mutated to alanine to inhibit further reaction after it had interacted with TXNIP (Figure 1b and c).

Purification of the T-TXNIP-TRX complex and its variants

Unluckily, we encountered an aggregation phenomenon during purification of the high concentration T-TXNIP-TRX complex. This was probably caused by non-specific covalent oligomerization between cysteine residues in the two proteins. To avoid such non-specific interactions, cysteine residues that are non-functional in the interaction between TXNIP and TRX (Patwari et al., 2006) were substituted with serine in series (Figure 1b and c). As a result, mutations of the Cys120, Cys170, Cys205 and Cys267 residues in T-TXNIP to serine resulted in stable complex formation (Figure 1c and Figure 2a). Although the complex containing mutation of the Cys63 residue to serine in T-TXNIP was also purified suitably (Figure 2a), it turned out that the residue is critical for maintaining the complex stable (see below). Size exclusion chromatographic (SEC) analysis with the purified protein complexes (~45 kDa) revealed that TXNIP (35 kDa) formed a stable and monodisperse protein complex with TRX (12 kDa) in solution and that the stoichiometry of the interaction between T-TXNIP and TRX is 1:1. As mentioned above, the T-TXNIP-TRX complex dissociated during SEC analysis, while the T-TXNIP-TRX(C35A) complex was firmly maintained (Figure 2b). The dissociation phenomenon between TXNIP and TRX was observed under oxidation conditions (Zhou et al., 2010). An oxidation of the T-TXNIP-TRX complex during the SEC analysis might induce the dissociation. Among the protein complexes, the T-TXNIP(C120S/C170S/C205S/C267S)-TRX(C35A) complex had the highest stability and lowest dispersity (Figure 2b).

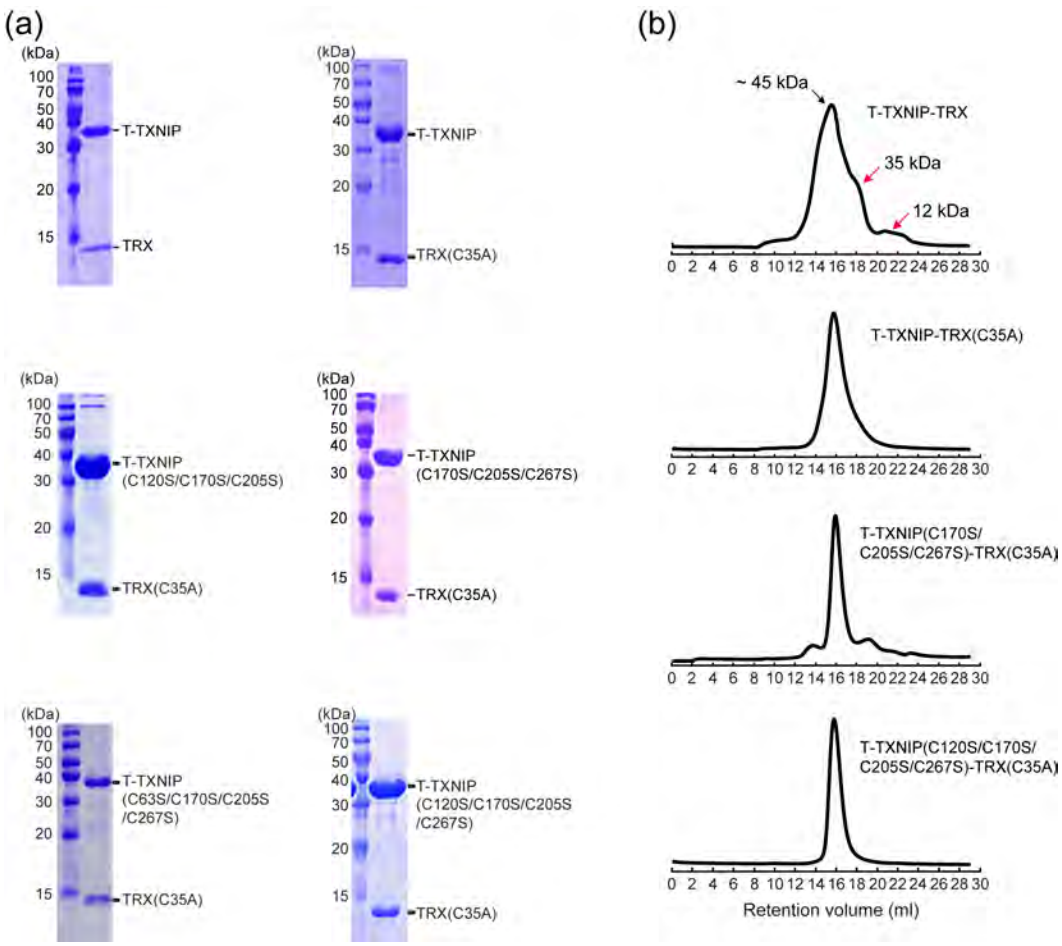

FIGURE 2 | The purified T-TXNIP-TRX complex and its variants. (a) SDS-PAGE analysis of the purified complexes to evaluate their homogeneity. (b) Size exclusion chromatographic analysis of the purified complexes. The red arrows indicate free forms of T-TXNIP and TRX. Figure 2b was adapted from previously published data (Hwang et al., 2014).

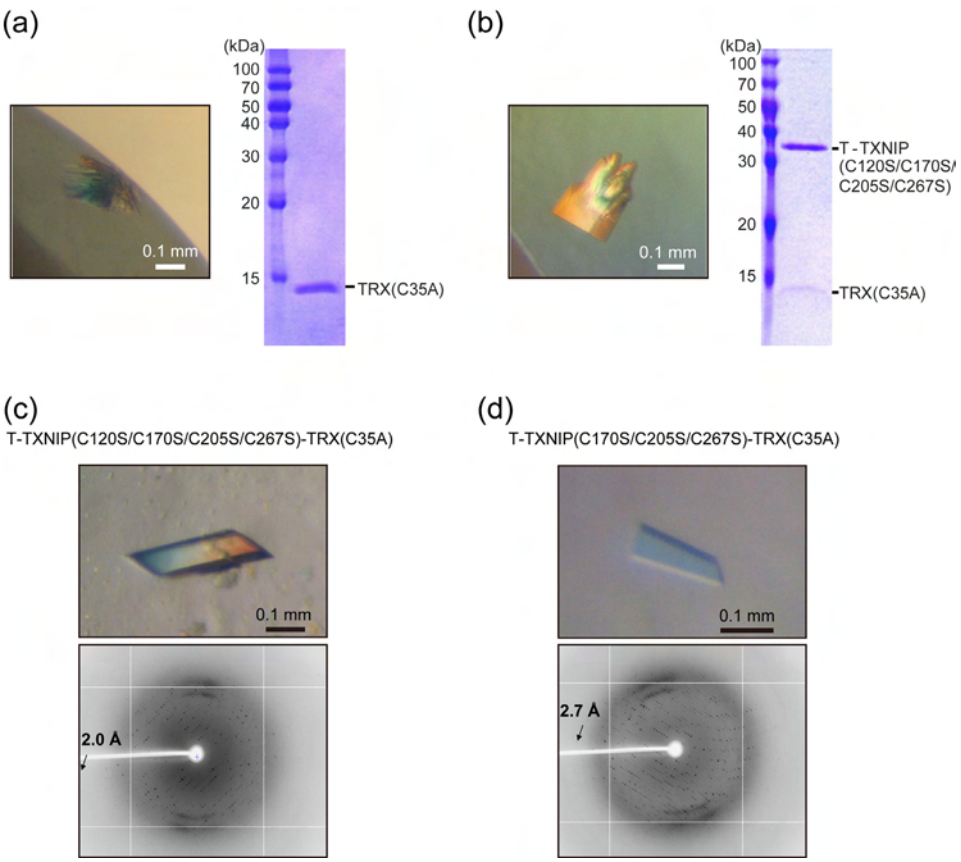

FIGURE 3 | Evaluation of the initial crystal hits and optimization to X-ray diffraction quality. (a,b) Initial crystal hits of different protein complexes were analyzed by SDS-PAGE. (c,d) Optimized complex crystals and X-ray diffraction snap-images. The optimized crystals of the T-TXNIP(C120S/C170S/C205S/C267S)-TRX(C35A) and T-TXNIP(C170S/C205S/C267S)-TRX(C35A) complexes diffracted to 2.0 Å (c) and 2.7 Å (d) resolution, respectively.

Crystallization of the protein complexes

The purified T-TXNIP-TRX(C35A) complex and its variants were crystallized and initial crystal hits were obtained from the T-TXNIP(C170S/C205S/C267S)-TRX(C35A), T-TXNIP(C63S/C170S/C205S/C267S)-TRX(C35A), and T-TXNIP(C120S/C170S/C205S/C267S)-TRX(C35A) complexes in different conditions (Figure 3). However, SDS-PAGE analysis revealed that the crystal of the T-TXNIP(C63S/C170S/C205S/C267S)-TRX(C35A) complex only contained TRX (Figure 3a), indicating that the Cys63 residue is crucial for interacting with TRX. The crystal of the T-TXNIP(C120S/C170S/C205S/C267S)-TRX(C35A) complex evidently showed both proteins (Figure 3b). The crystals of the T-TXNIP(C120S/C170S/C205S/C267S)-TRX(C35A) and T-TXNIP(C170S/C205S/C267S)-TRX(C35A) complexes were optimized to single crystals to be of a suitable quality for X-ray diffraction (Figure 3c and d). Crystals of both complexes appeared in a similar crystallization condition, namely, 0.12–0.16 M trisodium citrate and 16–18% PEG 3350.

Data collection and preliminary X-ray analysis

The optimized crystals of the T-TXNIP(C120S/C170S/C205S/C267S)-TRX(C35A) complex diffracted to 2.0 Å resolution (Figure 3c). The crystals belong to a primitive monoclinic system (space group $P2_1$) with unit-cell parameters of a=80.14 Å, b=64.02 Å, c=88.30 Å, and β =91.28°. The calculated Matthews coefficient (V_m) was 2.65 Å^3/Da, with a solvent content of 53.57%, indicating that there are two complex molecules in the asymmetric unit. The T-TXNIP(C170S/C205S/C267S)-TRX(C35A) complex diffracted to 2.7 Å resolution (Figure 3d) and showed the same space group as that of the T-TXNIP(C120S/C170S/C205S/C267S)-TRX(C35A) complex, with unit-cell parameters of a=79.83 Å, b=64.99 Å, c=88.42 Å, and β=90.88°. The calculated Vm and solvent content were 2.68 Å^3/Da and 54.15%, respectively. Data statistics are shown in the previously published paper (Hwang et al., 2014).

CONCLUSIONS

The redox-dependent TXNIP and TRX regulatory system is involved in many cellular processes including glucose and lipid metabolic signaling, cell growth and proliferation, and inflammatory signaling. Therefore, elucidation of the regulatory mechanism between the redox proteins TRX and TXNIP is critical to understand these cellular events, and structural study of the interaction between TXNIP and TRX is essential to uncover this mechanism. As a first step to achieving this goal, we described how the problematic redox protein complex of TXNIP and TRX can be overexpressed, purified, and crystallized. It turned out that both proteins are expressed as a soluble complex in the *E. coli* Rosetta-gami (DE3) system in which disulfide bonds can form owing to trxB/gor mutation. Moreover, stable complex proteins were obtained by catching TXNIP in a steady intermediate state in which TRX was bound. Eventually, non-functional cysteine-to-serine substitutions in TXNIP resulted in a successful crystallization of the complex.

METHODS

DNA cloning and mutagenesis

The co-expression plasmid to produce the T-TXNIP and TRX complex was constructed as described in the main text in detail. In this construct, T-TXNIP and TRX were independently expressed under the control of the trc promoter and the T7 promoter, respectively. A series of mutations were introduced into the T-TXNIP and TRX complex using the QuikChange Mutagenesis Kit (Stratagene), according to the manufacturer's instructions. All constructs were confirmed by sequencing.

Protein expression and purification

E. coli Rosetta gami (DE3) cells harboring the overexpression plasmids were grown in LB medium containing ampicillin at 37°C until the optical density at 600 nm reached between 0.4 and 0.6. Thereafter, the temperature was reduced to 21°C and expression of the wild-type T-TXNIP-TRX complex and its variants was induced by the addition of isopropyl-β-D-thiogalactopyranoside to a final concentration of 0.5 mM for 40 h. The cells were harvested by centrifugation at 5,000×g at 4°C for 15 min, and cell pellets were resuspended in cooled buffer A (50 mM Tris-HCl, pH 8.0, 500 mM NaCl, and 10% glycerol) supplemented with 1 mM dithiothreitol (DTT) to prevent the dissociation between T-TXNIP and TRX under oxidation conditions (Zhou et al., 2010). The resuspended cells were disrupted by ultrasonication. The cell debris containing insoluble material and the soluble fraction containing the protein complex were separated by centrifugation at 20,000×g at 4°C for 1 h. The supernatant including the His-tagged complex protein was loaded onto a Ni-NTA agarose (Qiagen) column pre-equilibrated with buffer A. The column was intensively washed with buffer A containing 30 mM imidazole and 1 mM DTT, and the complex was eluted using buffer A containing 500 mM imidazole. The rTEV protease (GIBCO) was added to the elution fraction at a 1:100 ratio to release the His-tag from the T-TXNIP-TRX complex, and the mixture was incubated at 4°C overnight. The T-TXNIP-TRX complex was then concentrated and purified by size-exclusion chromatography. A Superdex 200 10/300 GL gel filtration column (GE Healthcare) installed on an AKTA purifier FPLC system (GE Healthcare) was equilibrated with buffer A at a flow rate of 0.3 ml/min at room temperature. The protein solution including rTEV protease was injected into the column. The fractions containing the T-TXNIP-TRX complex were collected and applied to a Ni-NTA agarose column for further purification. The flow-through fraction containing the T-TXNIP-TRX complex was concentrated using an Amicon-15 10K concentrator to a final concentration of 12–15 mg/ml for crystallization.

Crystallization and preliminary X-ray analysis

Initial crystal screening was performed with the purified complexes of T-TXNIP-TRX, T-TXNIP-TRX(C35A), T-TXNIP(C120S/C170S/C205S)-TRX(C35A), T-TXNIP(C170S/C205S/C267S)-TRX(C35A), T-TXNIP(C63S/C170S/C205S/C267S)-TRX(C35A), and T-TXNIP(C120S/C170S/C205S/C267S)-TRX(C35A) using the sitting-drop vapor-diffusion method at 21°C. Initial crystals from T-TXNIP(C63S/C170S/C205S/C267S)-TRX(C35A) were generated in 0.1 M sodium acetate trihydrate, pH 4.6, and 2.0 M ammonium sulfate, and those from T-TXNIP(C120S/C170S/C205S/C267S)-TRX(C35A) and T-TXNIP(C170S/C205S/C267S)-TRX(C35A) were generated in 0.16 M tri-ammonium citrate and 18% PEG 3350. SDS-PAGE analysis revealed that the T-TXNIP(C63S/C170S/C205S/C267S)-TRX(C35A) crystal contained only TRX. Optimal crystals of T-TXNIP(C120S/C170S/C205S/C267S)-TRX(C35A) and T-TXNIP(C170S/C205S/C267S)-TRX(C35A) appeared in 0.12–0.16 M tri-sodium citrate and 16–18% (w/v) PEG 3350. The crystals of the T-TXNIP(C120S/C170S/C205S/C267S)-TRX(C35A) complex, which were frozen in a cryosolution consisting of 0.16 M tri-sodium citrate, 16% PEG 3350, and 25% glycerol, diffracted to 2.0 Å resolution at beamline 4A in the Pohang Accelerator Laboratory (PAL). The crystals of the T-TXNIP(C170S/C205S/C267S)-TRX(C35A) complex frozen in the same cryosolution as that of the T-TXNIP(C120S/C170S/C205S/C267S)-TRX(C35A) complex diffracted to 2.7 Å resolution at the same beamline. All diffraction data were processed and scaled using the HKL2000 software package (Otwinowski and Minor, 1997).

ACKNOWLEDGMENTS

We thank the staff of the macromolecular X-ray crystallography beamlines, PAL, Korea, for their help with data collection. This work was supported by the Global Frontier Project (NRF-2010-0029767) funded by the Ministry of Science, ICT and Future Planning, Korea, and by the KRIBB Research Initiative Program.

AUTHOR INFORMATION

The authors declare no potential conflicts of interest.

Original Submission: May 1, 2014
Revised Version Received: May 25, 2014
Accepted: May 26, 2014

REFERENCES

Alvarez, C.E. (2008). On the origins of arrestin and rhodopsin. *BMC Evol Biol* **8**, 222.

Choi, A.M., and Nakahira, K. (2011). Dampening insulin signaling by an NLRP3 'meta-flammasome'. *Nat Immunol* **12**, 379-80.

Dunn, L.L., Buckle, A.M., Cooke, J.P., and Ng, M.K. (2010). The emerging role of the thioredoxin system in angiogenesis. *Arterioscler Thromb Vasc Biol* **30**, 2089-98.

Hwang, J., Suh, H.W., Jeon, Y.H., Hwang, E., Nguyen, L.T., Yeom, J., Lee, S.G., Lee, C., Kim, K.J., Kang, B.S., Jeong, J.O., Oh, T.K., Choi, I., Lee, J.O., and Kim, M.H. (2014). The structural basis for the negative regulation of thioredoxin by thioredoxin-interacting protein. *Nat Commun* **5**, 2958.

Lillig, C.H., and Holmgren, A. (2007). Thioredoxin and related molecules--from biology to health and disease. *Antioxid Redox Signal* **9**, 25-47.

Mukherjee, A., and Martin, S.G. (2008). The thioredoxin system: a key target in tumour and endothelial cells. *Br J Radiol* **81**, S57-68.

Otwinowski, Z., and Minor, W. (1997). Processing of X-ray Diffraction Data Collected in Oscillation Mode. *Methods Enzymol* **276**, 307-26.

Patwari, P., Higgins, L.J., Chutkow, W.A., Yoshioka, J., and Lee, R.T. (2006). The interaction of thioredoxin with Txnip. Evidence for formation of a mixed disulfide by disulfide exchange. *J Biol Chem* **281**, 21884-91.

Powis, G., and Kirkpatrick, D.L. (2007). Thioredoxin signaling as a target for cancer therapy. *Curr Opin Pharmacol* **7**, 392-7.

Schroder, K., Zhou, R., and Tschopp, J. (2010). The NLRP3 inflammasome: a sensor for metabolic danger? *Science* **327**, 296-300.

Schulze, P.C., Yoshioka, J., Takahashi, T., He, Z., King, G.L., and Lee, R.T. (2004). Hyperglycemia promotes oxidative stress through inhibition of thioredoxin function by thioredoxin-interacting protein. *J Biol Chem* **279**, 30369-74.

Schutze, N., Bachthaler, M., Lechner, A., Kohrle, J., and Jakob, F. (1998). Identification by differential display PCR of the selenoprotein thioredoxin reductase as a 1 alpha,25(OH)2-vitamin D3-responsive gene in human osteoblasts--regulation by selenite. *Biofactors* **7**, 299-310.

Spindel, O.N., World, C., and Berk, B.C. (2012). Thioredoxin interacting protein: redox dependent and independent regulatory mechanisms. *Antioxid Redox Signal* **16**, 587-96.

Tagaya, Y., Maeda, Y., Mitsui, A., Kondo, N., Matsui, H., Hamuro, J., Brown, N., Arai, K., Yokota, T., and Wakasugi, H. (1989). ATL-derived factor (ADF), an IL-2 receptor/Tac inducer homologous to thioredoxin; possible involvement of dithiol-reduction in the IL-2 receptor induction. *EMBO J* **8**, 757-64.

Yoshihara, E., Chen, Z., Matsuo, Y., Masutani, H., and Yodoi, J. (2010). Thiol redox transitions by thioredoxin and thioredoxin-binding protein-2 in cell signaling. *Methods Enzymol* **474**, 67-82.

Zhou, R., Tardivel, A., Thorens, B., Choi, I., and Tschopp, J. (2010). Thioredoxin-interacting protein links oxidative stress to inflammasome activation. *Nat Immunol* **11**, 136-40.

